PROCEEDINGS OF SCIENCE

Fourth generation searches at ATLAS

Snežana Nektarijević[*†]
Université de Genève
E-mail: snezana.nektarijevic@cern.ch

Thanks to the outstanding LHC accelerator and ATLAS detector performances, 4.7 fb^{-1} of pp collision data with centre of mass energy 7 TeV were recorded in 2011. This has allowed for precision measurements but also searches for new physics. The searches for the fourth sequential generation quarks t' and b' using 1 fb^{-1} of ATLAS data are presented. No excesses of events above the Standard Model prediction were observed and lower limits on the t' and b' quark masses at 95% C.L. have been placed.

The XIth International Conference on Heavy Quarks and Leptons,
June 11-15, 2012
Prague, Czech Republic

[*]Speaker.
[†]On behalf of the ATLAS Collaboration.

PoS(HQL 2012)070

1. Introduction

The Standard Model (SM) of particle physics with three generations of quarks and leptons leads to a handful of open questions which need to be addressed by new physics models. A natural extension of the SM would be a fourth chiral generation of quarks. Extending the CKM matrix to 4×4 could generate additional CP violation, potentially sufficient to explain the baryon asymmetry while providing further insights into the forward-backward asymmetry in production of top-antitop pairs, the quark mass hierarchy and dark matter [1].

The existence of the fourth generation is theoretically and experimentally allowed. QCD allows up to eight quark generations and the global fit to the electroweak precision data (Fig. 1) allows for at least one additional generation in case $m_{t'} - m_{b'} < m_W$ and $m_{b'} > m_t + m_W$. Thus, in the analyses presented only the decay modes $t' \to Wq$ and $b' \to Wt \to WWb$ are considered.

The excellent Large Hadron Collider (LHC) accelerator performance in 2011 offers enough data for searches for fourth generation. Four direct searches for fourth generation quarks, carried out by the ATLAS Collaboration, are presented. Although the fourth generation model has been used as a bench mark, results presented can also be interpreted in terms of the exclusion limits on other models, e.g. the vector-like-quarks.

2. ATLAS Detector

ATLAS [2] is a 44 m long cylindrical detector 25 m in diameter (Fig. 2). It consists of the inner detector surrounded by a superconducting solenoid magnet, the electromagnetic and hadronic calorimeters and the muon spectrometer. The inner detector, consisting of pixel and silicon microstrip detectors and a transition radiation tracker immersed in a 2 T axial magnetic field, provides charged particle tracking in the pseudorapidity region $|\eta| < 2.5$. The electromagnetic calorimeter, made of lead and liquid argon, and the hadron calorimeter, with scintillator tiles and liquid argon as active material and with steel, copper or tungsten as the absorber material, provide energy deposit measurements up to $|\eta| < 4.9$. The muon spectrometer, placed inside air-core toroids producing a field strength of $2.5-6.0$ T, contains a system of trigger chambers covering up to $|\eta| < 2.4$ and high precision tracking chambers covering up to $|\eta| < 2.7$.

3. Event Topology Reconstruction

The final states of t' and b' pair production contain two and four W bosons respectively. Since a W boson decays to hadrons with branching fraction of 67.6%, in the largest fraction of events only jets are produced. Such events are however difficult to distinguish from the large multijet production events. It is experimentally more convenient to look for signatures with at least one W boson decaying into a lepton-neutrino pair, lepton being either an electron or a muon (since the events with taus have higher background rates). Thus the selected events need to include isolated leptons (electrons or muons), jets and high missing transverse energy ($E_{\mathrm{T}}^{\mathrm{miss}}$) due to neutrinos.

Electron candidates need to satisfy have transverse momentum $p_{\mathrm{T}} > 25$ GeV (unless otherwise stated) and $|\eta| < 2.47$, excluding $1.37 < |\eta| < 1.52$, the transition region between the barrel and endcap electromagnetic (EM) calorimeters. Muon candidates need to fulfill $p_{\mathrm{T}} > 20\,\mathrm{GeV}$ and

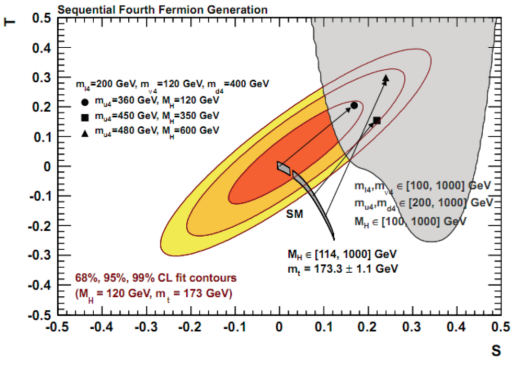

Figure 1: The SM electroweak fit and the fourth generation prediction in the space of the Peskin-Takeuchi oblique parameters S and T provided by the Gfitter Group [4].

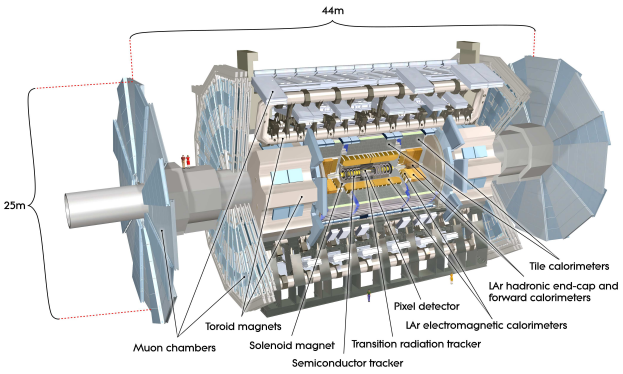

Figure 2: ATLAS detector layout [2].

$|\eta| < 2.5$. The p_{T} requirement ensures that the selected leptons are in the efficiency plateau of the single-lepton triggers.

The $E_{\mathrm{T}}^{\mathrm{miss}}$ is calculated as the vector sum of all calorimeter cells contained in topological clusters including contributions from selected muons and calibrated at the energy scale of the associated high-p_{T} object.

Selected jets are required to satisfy $p_{\mathrm{T}} > 25$ GeV (except in Sec. 10 where $p_{\mathrm{T}}^{\mathrm{jet}} > 20$ GeV is required) and $|\eta| < 2.5$. The jets are reconstructed with the anti-kt algorithm with radius parameter R = 0.4, from topological clusters of energy deposits in the calorimeters calibrated at the EM scale. These jets are then calibrated to the particle level using a p_{T}- and η-dependent correction factor derived from simulated events and validated using data. In some analyses a certain number of jet is required to be identified as originating from the hadronization of a b quark. The identification of such jets, called b-tagging, is performed using multivariate techniques combining information from the impact parameters of displaced tracks and topological properties of secondary and tertiary decay vertices reconstructed within the jet [3]. The chosen working point has 70% efficiency for b-quark jets and a rejection factor of 100 for jets originating from light quarks (u, d, s) or gluons.

4. Data and Monte Carlo Samples

The analyses presented have been carried out with the data set taken by the ATLAS experiment between March and June 2011 using single electron and muon triggers. Only the events collected under stable beam conditions and for which all detector subsystems were fully operational have been included. The corresponding integrated luminosity is 1.04 fb^{-1}.

The t' and b' signal is estimated from Monte Carlo (MC) simulation generated with Pythia 6.421 [5] and normalized to their approximate to next-to-next-to-leading-order (NNLO) theoretical cross section calculated using HATHOR [6]. The quark decays with subsequent showering and hadronization have been generated with Pythia for a quark mass range from 200 to 600 GeV for t' and from 300 to 600 GeV for b', in steps of 50 GeV in both cases. The CTEQ6.6 [7] parton distribution functions (PDF) is used for t' and MRST2007 LO* [8] for b'. The $t\bar{t}$ and single top quark

background MC samples are generated using MC@NLO v3.41[9] (except in Sec. 9 where Alpgen [10] is used), assuming a top quark mass of 172.5 GeV, using the CTEQ6.6 PDF set and are normalized to the approximate NNLO theoretical cross sections. The W/Z+jets background samples are generated using Alpgen v2.13 [10] and the CTEQ6L1 [11] PDF set. The Z+jets background is normalized to its NNLO theoretical cross section, while the W+jets background normalization is extracted from data. Both MC@NLO and Alpgen are interfaced to Herwig v6.5 [12] to model the parton shower and fragmentation, while the underlying event is simulated by Jimmy [13]. The diboson backgrounds are modeled using Herwig and normalized to their NLO theoretical cross sections. The $t\bar{t}$+bosons samples ($t\bar{t}W$, $t\bar{t}Z$, $t\bar{t}WW$, $t\bar{t}Wj$, $t\bar{t}Zj$) as well as $WWjj$ are generated by MadGraph and interfaced to Pythia for showering and hadronization.

All MC samples include multiple pp interactions and are processed through a full simulation [14] of the ATLAS detector geometry and response using Geant4 [15], and the same reconstruction software as the data. Simulated events are corrected to match the object identification efficiencies and resolutions determined in data control samples.

5. Systematic Uncertainties

Systematic uncertainties affecting the shape and normalization of the discriminant distributions are estimated for both signal and backgrounds. The sources of the systematic uncertainties are mostly the same among all four analyses presented although their sensitivity to them is different.

The delivered luminosity is calibrated with the dedicated van der Meer scans and the associated uncertainty is estimated to be $\delta L/L = \pm 3.7\%$ [16]. The multiple pp interaction uncertainty is found to have a very small effect on the result.

The dominant $t\bar{t}$ background is affected by various sources of uncertainties: the theoretical uncertainty on the cross section is $(^{+7.0}_{-9.6}\%)$; the normalization and the shape of the discriminants are affected by the uncertainties on the fragmentation model (based on the comparison of Herwig and Pythia fragmentations), on the NLO event generator (based on the comparison of the prediction from Powheg [17] with Herwig and Alpgen in Sec. 9 or prediction from MC@NLO with Powheg otherwise) and on the top quark mass (taken to be ± 1 GeV).

The uncertainty on the jet energy scale (JES) affects the normalization of signal and backgrounds modeled through the simulation, as well as the shape of the distributions used.

Uncertainties on the modeling of initial- and final-state QCD radiation (ISR/FSR) is evaluated by varying corresponding generator parameters, and is considered as correlated between the $t\bar{t}$ background and the $t'\bar{t}'$ signal.

The uncertainties on the normalization of the W+jets background are derived from measurements of W+2 jets final state. The uncertainty on the heavy-flavor content of the samples and the extrapolation to higher jet multiplicities are taken into account. Uncertainties on the shape of the discriminating distributions for the W+jets background are estimated by varying the chosen matching scale (from 15 to 10 GeV) and the factorization scale (from $\mu_F^2 = m_W^2 + \sum p_{T,jet}^2$ to $\mu_F^2 = m_W^2 + p_{T,W}^2$) in Alpgen.

Uncertainties on the b-tagging algorithms affect the identification of b/c-jets as well as the misidentification of light jets.

The Z+jets, single top and diboson backgrounds are varied within the uncertainty on their theoretical cross sections. The uncertainty on the multi-jet background event normalizations is conservatively taken to be 100% and the uncertainties on its shape are estimated by varying the lepton identification criteria used in the extraction method.

6. Limit Setting

In the absence of any significant excess of events in data with respect to the SM prediction, 95% confidence level (C.L.) upper limits on the production cross section of the considered quark are derived using the CL_S method [18] using an *LLR* test-statistic. Pseudo-experiments are generated assuming both the signal-plus-background (s+b) and background-only (b). The per-bin statistical fluctuations of the total predictions are taken into account according to Poisson statistics and the fluctuations in the signal and background expectations due to systematic uncertainties are treated as Gaussian. CL_{s+b} and CL_b for the observed (expected) limits are defined by the fraction of $s+b$ and b pseudo-experiments with *LLR* larger than the observed (median) *LLR*. Signal cross sections for which $CL_S = CL_{s+b}/CL_b < 0.05$ are considered excluded at the 95% C.L.

7. Search for t' in Single Lepton Final State [21]

$t'\bar{t}'$ events in the lepton+jets channel are required to contain exactly one lepton (e or μ), at least three jets and significant E_T^{miss}. The requirement of $E_T^{miss} > 35(20)$ GeV for the electron (muon) channel is combined with $E_T^{miss} + m_T^W > 60$ GeV, where m_T^W is the transverse mass[1] of the lepton-neutrino system, in order to suppress the multi-jet production background. At least one jet is required to have $p_T > 60$ GeV and at least one needs to be b-tagged.

The dominant background after event selection is $t\bar{t}$ production followed by W+jets production. Other smaller contributions come from multi-jet, single top, Z+jets and diboson production. Multi-jet events contain a jet or a photon which is misidentified as an electron or a non-prompt lepton e.g. from semileptonic b- or c-hadron decays. Their contribution is estimated by a data driven matrix method [19]. The W+jets background normalization is estimated from the measurement of the asymmetry between W^++jets and W^-+jets production in data while its shape is estimated from simulation. The other backgrounds and the signal are estimated from the simulation and normalized to their theoretical cross sections.

The primary discriminant of the analysis is the reconstructed heavy quark mass, m_{reco}. In events with at least four jets, m_{reco} is constructed using a kinematic likelihood fit [20] to the $t'\bar{t}' \to W^+bW^-b \to l\nu bq\bar{q}'\bar{b}$ hypothesis (Fig. 3). In events with exactly three jets, m_{reco} is constructed as the invariant mass of the three jet system.

The m_{reco} distribution is analysed with a binned log-likelihood ratio $LLR = -2\log(L_{s+b}/L_b)$ as test-statistic, L_{S+B} (L_b) being a Poisson likelihood of observing the data given signal-plus-background (background-only) hypothesis. The L_{s+b} and L_b are parametrized in terms of 12 nuisance parameters which describe the effects of the leading sources of uncertainties, such as JES, ISR/FSR, and normalizations of $t\bar{t}$, W+jets and multi-jet production. Both likelihood functions

[1] The transverse mass of the lepton-neutrino system is defined as $m_T^W = \sqrt{2E_T^{miss}p_T^l\left(1-\cos\left(\Delta\phi\left(E_T^{miss},p_T^l\right)\right)\right)}$

are minimized with respect to the nuisance parameters allowing the data to constrain some of the leading systematic uncertainties.

In absence of any significant excess of events in data above the SM prediction the 95% C.L. upper limits on the $t'\bar{t}'$ production cross section as a function of t' quark mass have been derived using the CL_S method (shown in Fig. 4). This translates into an observed (expected) lower limit of 404 (394) GeV on the t' quark mass.

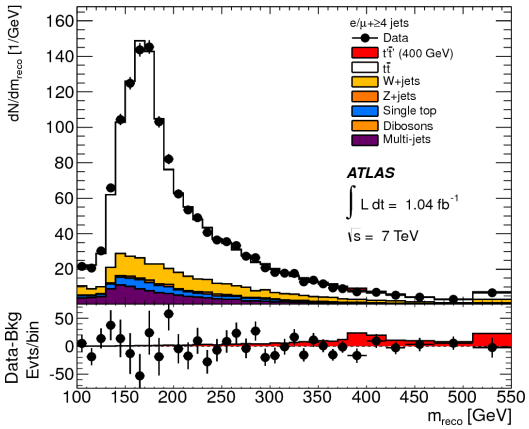

Figure 3: Reconstructed t' mass in events with at least 4 jets [21].

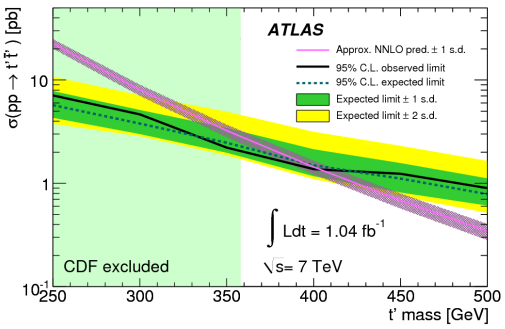

Figure 4: $t'\bar{t}'$ production cross-section as a function of the t' quark mass[21].

8. Search for heavy Q in Opposite-Sign Diepton Final State [22]

This search targets the pair production of a heavy quark Q with the decay mode $Q \to Wq$, where $q = u,d,s,c$ or b. The SM t' quark is used as the benchmark. The process considered is $Q\bar{Q} \to l^+\nu q l^-\bar{\nu}\bar{q}$, l being an electron or a muon. The signature of the process contains at least two jets, two oppositely charged leptons and significant $E_{\mathrm{T}}^{\mathrm{miss}}$ arising from two undetected neutrinos.

Selected events need to contain exactly two leptons (e or μ) with opposite charges and two or more jets. In order to suppress the Drell-Yan background which is dominant at this stage, one needs to ask for jets with $p_{\mathrm{T}} > 25$ GeV and $|\eta| < 2.5$, and $E_{\mathrm{T}}^{\mathrm{miss}} > 60$ GeV. Furthermore, the dilepton invariant mass m_{ll} must be greater than 15 GeV and outside of the Z boson window (81 GeV, 101 GeV) in the same-flavor events (ee or $\mu\mu$), and for the different-flavor events ($e\mu$) the scalar sum of transverse energy from every lepton and jet passing the object selection, H_{T}, must be greater than 130 GeV.

The total number of Drell-Yan ee and $\mu\mu$ events is estimated with a data-driven method which extrapolates from the control regions, whereby the non-Drell-Yan events are subtracted from the data using simulation. The fraction of the non-prompt leptons misidentified as prompt leptons from W boson decays is determined by the data-driven matrix method technique.

The main discriminant of the analysis is the heavy-quark mass reconstructed in such a way to take advantage of the larger boost of the W bosons in signal events compared to the dominant $t\bar{t}$ background. It is assumed that $E_{\mathrm{T}}^{\mathrm{miss}}$ fully arises from two neutrinos which are approximately

collinear with their leptonic partners. The optimal angles $|\Delta\eta\,(\nu,l)|$ and $|\Delta\phi\,(\nu,l)|$ are fit by minimizing the mass difference between the two reconstructed heavy quarks. The fitted neutrino direction is constrained to be within the space angle [2] $\Delta R < 2.5$ around the corresponding lepton originating from the same W boson. The requirement on the invariant mass of the lepton-neutrino systems to be as close as possible to the nominal W boson mass is included in the fit as a term in the minimized function. The final reconstructed mass $m_{\text{Collinear}}$, an example of which is shown in Fig. 5, is the average of the two reconstructed heavy quark masses in the event. Final selection cuts are performed in the $m_{\text{Collinear}}$-$\left(H_{\text{T}} + E_{\text{T}}^{\text{miss}}\right)$ plane employing the differences in the correlations between the two variables for signal and the background.

The $m_{\text{Collinear}}$ rates for signal and background are fitted simultaneously to the observed data using binned maximum likelihood method in order to measure the most likely $Q\bar{Q}$ production cross-section. The shapes of the $m_{\text{Collinear}}$ distribution in signal and background pseudo-data are smoothly smeared by random variations consistent with the systematic uncertainties evaluated individually from either simulation or data-driven techniques, but not constrained by the data.

In absence of any excess of events in data over the SM prediction, the observed (expected) 95 % C.L. lower limit on the heavy quark mass is found to be $m_{\text{Q}} > 350\,(335)$ GeV (Fig. 6).

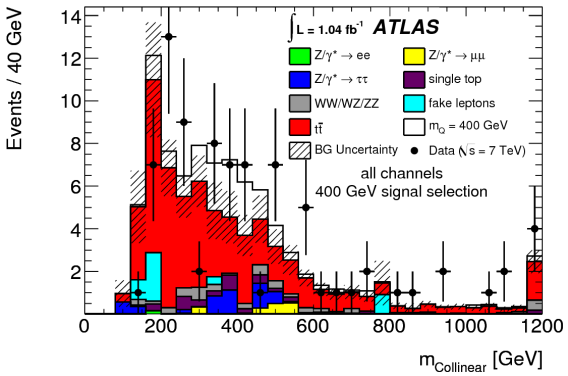

Figure 5: Collinear mass distribution [22].

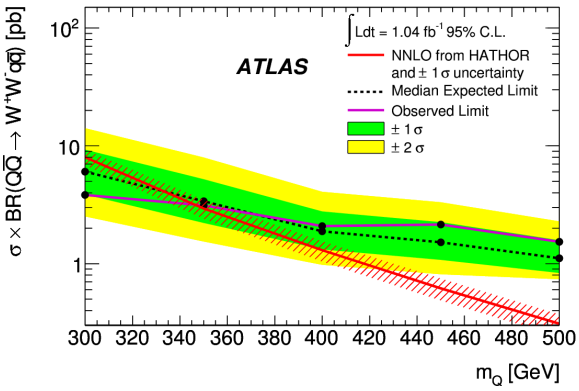

Figure 6: $t't'$ production cross-section as a function of the t' quark mass [22].

9. Search for b' in Single Lepton Final State [23]

The search for pair production of a fourth generation down-type quark b' in events with one lepton is presented here. In the model where b' is a chiral quark with mass larger than $m_t + M_W$, the predominant decay mode is $b' \to Wt \to WWb$, which leads to four W bosons and two b quarks in the $b'\bar{b}'$ production events.

Due to the high expected b' mass, the W bosons coming from the $b' \to Wt$ decay are expected to have a high momentum and the decay products of such W bosons should be closer than jets for background processes, but still resolvable as separate jets with spatial separation $\Delta R \approx 2m_W/p_{\text{T}}^W$. Considering this, the quantity suitable for distinguishing b' signal from background is the number of jet pairs with small opening angle and an invariant mass close to the W boson mass.

[2] Space angle $\Delta R = \sqrt{\Delta\eta^2 + \Delta\phi^2}$

The dominant background in this analysis is the $t\bar{t}$ production with additional jets. The second largest contribution is due to W+jets production. Prediction of these backgrounds are significantly affected by the theoretical uncertainties on the level of gluon radiation and experimental uncertainties on jet energy scale and resolution. The other backgrounds are due to single top production, diboson production (WW, WZ, ZZ), Z+jets events in which a lepton is not detected and multi-jet production with one jet being misidentified as a lepton.

The final state signature of the decay contains exactly one lepton (e or μ), $E_{\mathrm{T}}^{\mathrm{miss}}$ and at least six jets passing the object selection. To reduce the multi-jet background additional selection is required: $E_{\mathrm{T}}^{\mathrm{miss}} > 35$ GeV and $m_{\mathrm{T}}^{W} > 25$ GeV in the events with an electron, and $E_{\mathrm{T}}^{\mathrm{miss}} > 20$ GeV and $E_{\mathrm{T}}^{\mathrm{miss}} + m_{\mathrm{T}}^{W} > 60$ GeV in the events with a muon.

The quantity of interest is the number of reconstructed W bosons (N_W) defined as the number of the pairs of jets separated by $\Delta R < 1.0$ with an invariant mass in the range $70 - 100$ GeV. The final discriminant consists of nine exclusive bins as a function of the multiplicity of hadronic W decays ($N_W = 0, 1, \geq 2$) and jet multiplicity ($N_{\mathrm{jet}} = 6, 7, \geq 8$), as shown in Fig. 7.

The most likely value of the $b'\bar{b}'$ cross section in the nine bins of (N_W, N_{jet}) multiplicity is extracted with a binned maximum likelihood fit using a profile likelihood ratio, varying each background rate within its uncertainty, and allowing shape and rate variation due to the systematic uncertainties. The signal and background rates are fitted simultaneously.

No evidence of b' quark production is observed, so the 95 % C.L. exclusion limit is set on the b' pair production cross section as a function of the b' quark mass employing th CL_S method. This translates into an observed (expected) lower bound on the b' quark mass of 480 (470) GeV, as illustrated in Fig. 8.

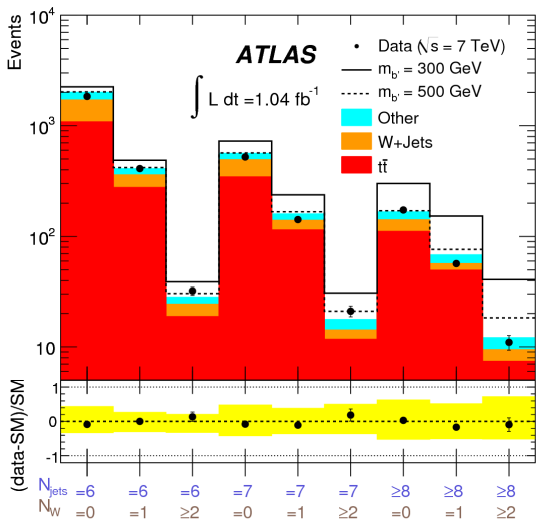

Figure 7: Nine analysis bins of N_W, N_{jet} [23].

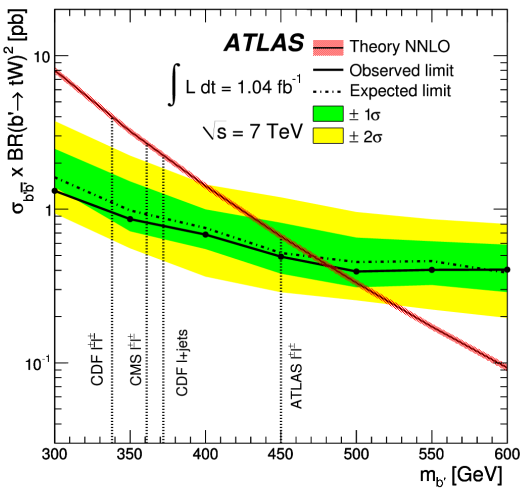

Figure 8: $b'\bar{b}'$ production cross-section as a function of the b' quark mass [23].

10. Search for b' in Same-Sign Dilepton Final State [24]

This is a search for an excess of events in final states containing two leptons of the same

charge. This signature has a low background rate in the SM but potentially large contribution from new physics theories, such as e.g. the flavor-changing Z boson proposed to explain the forward-backward asymmetry in $t\bar{t}$ events. Two processes leading to this final state signature are considered: same-sign top-quark production and pair production of down-type heavy quarks, using the fourth generation chiral quark b' as the benchmark.

Selected events need to contain at least two leptons with the same electric charge within the detector acceptance. In case of multiple same-sign pairs, the pairs are sorted according to the leading lepton p_{T}. In the same-flavor pairs (ee or $\mu\mu$) the invariant mass of two leptons must exceed 15 GeV and be outside of the Z-boson mass window: $|m_{ll} - m_Z| > 10$ GeV. There must be at least two selected jets and $E_{\mathrm{T}}^{\mathrm{miss}} > 40$ GeV.

The SM backgrounds arise either from events in which one lepton originates from a jet (fake-lepton) or from a photon conversion, or from events in which the electric charge of one lepton is misidentified (charge-flip), or from events in which the same-sign leptons are coming from a pair of Z or W bosons. Except for the diboson contribution which is estimated from simulation, all other backgrounds are estimated by extrapolation from control regions in data.

The analysis uses the cut and count method in three regions (shown in Fig. 9):

- Heavy-quark signal region: heavy down-type quark pairs or same-sign top quark pairs coming from high-mass Z' exchange, described by $H_{\mathrm{T}} > 350$ GeV. The leptons are either both positively or both negatively charged.
- Same-sign top-quark signal region: the subset of the 'heavy-quark signal region' containing only positively charged lepton pairs since the pp initial state of the LHC produces predominantly positively charged top quarks.
- Low-mass Z' boson signal region: positively charged leptons, $H_{\mathrm{T}} > 150$ GeV and invariant dilepton mass $m_{ll} > 100$ GeV are required.

In all three region the number of observed events is in a good agreement with the SM prediction. The exclusion limit in terms of a 95 % C.L. lower bound on the b' mass is set at 450 GeV using the CL_{S} method (Fig. 10).

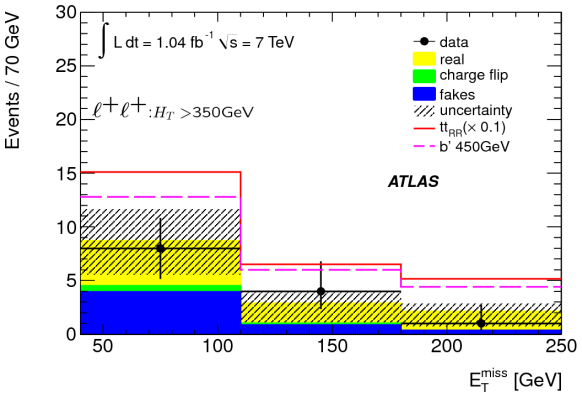

Figure 9: Three signal regions for positive same-sign leptons [24].

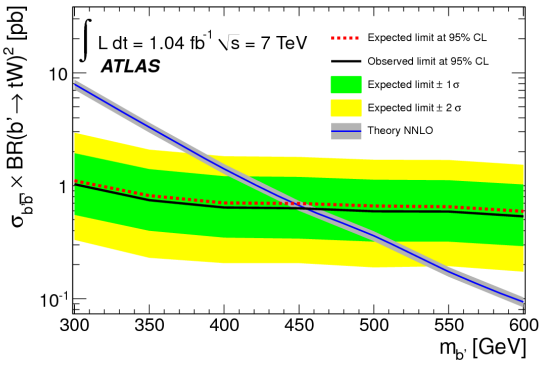

Figure 10: $b'\bar{b}'$ production cross-section as a function of the b' quark mass [24].

11. Conclusions

Searches for pair production of the fourth generation chiral quarks t' and b' with 1.04 fb^{-1} ATLAS pp-collision data were presented. No evidence of such processes has been observed and the 95 % C.L. exclusion limits have been derived using the CL_S method. The t' quark mass exclusion limit is 404 GeV in the single lepton and 350 GeV in opposite-sign dilepton final state. The b' quark is excluded for masses under 480 GeV in the single state and 450 GeV in the same-sign dilepton final state.

References

[1] B. Holdom et al., PMC Physics A 3, 4 (2009) and references therein.

[2] ATLAS Collaboration, J. Instrum. 3, S08003 (2008).

[3] ATLAS Collaboration, ATLAS-CONF-2011-102 (2011), https://cdsweb.cern.ch/record/1369219.

[4] M. Baak et al., Eur. Phys. J. C72 (2012) 2003

[5] T. Sjostrand, S. Mrenna, and P. Skands, JHEP 05 (2006) 026.

[6] M. Aliev et al., Comput. Phys. Commun. 182, 1034 (2011).

[7] P. M. Nadolsky et al., Phys. Rev. D 78, 013004 (2008).

[8] A. Sherstnev and R. Thorne, Eur. Phys. J. C 55, 553 (2008).

[9] S. Frixione, E. Laenen, P. Motylinski, C. White, and B. R. Webber, J. High Energy Phys. 2008, 029 (2008).

[10] M.L. Mangano et al., JHEP 0307, 001 (2003).

[11] J. Pumplin et al. JHEP 0207, 012 (2002).

[12] J. Campbell, R. K. Ellis, and D. Rainwater, Phys. Rev. D 68, 094021 (2003).

[13] J. Butterworth, J. Forshaw, and M. Seymour, Z. Phys. C 72, 637 (1996).

[14] ATLAS Collaboration, Eur. Phys. J. C 70, 823 (2010).

[15] The GEANT4 Collaboration, Nucl. Instrum. Methods Phys. Res., Sect. A 506, 250 (2003).

[16] ATLAS Collaboration, ATLAS-CONF-2011-116 (2011), https://cdsweb.cern.ch/record/1367408.

[17] P. Nason, J. High Energy Phys. 2004, 040 (2004).

[18] T. Junk, Nucl. Instr. Methods Phys. Res. A 434, 435 (1999); A. L. Read, J. Phys. G 28, 2693 (2002).

[19] ATLAS Collaboration, Eur. Phys. J. C 71, 1577 (2011).

[20] ATLAS Collaboration, (2012), Eur. Phys. J. C72 (2012) 2039

[21] ATLAS Collaboration, (2012), Phys.Rev.Lett. 108 (2012) 261802.

[22] ATLAS Collaboration, (2012), accepted for publication by Physical Review D, arXiv:1202.3389v1.

[23] ATLAS Collaboration, (2012), Phys. Rev. Lett. 109 (2012) 032001

[24] ATLAS Collaboration, (2012), JHEP 1204 (2012) 069, arXiv:1202.5520.